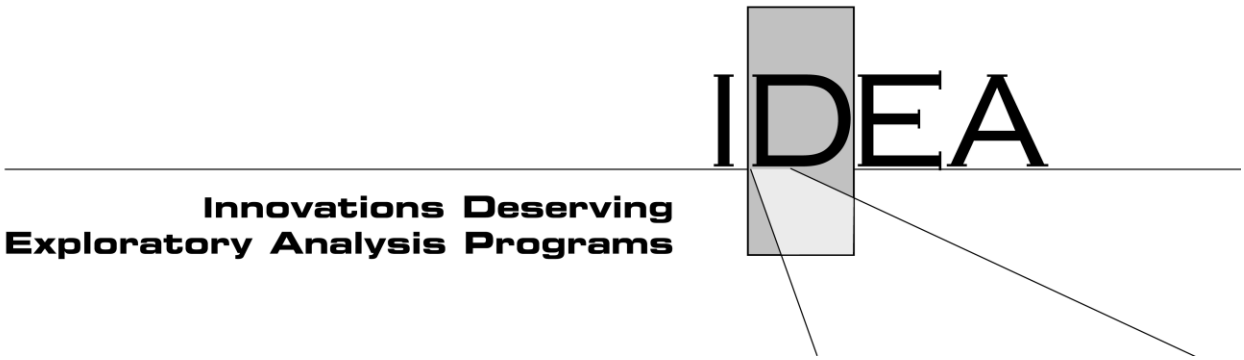

Highway IDEA Program

Extraction of Layer Properties from Intelligent Compaction Data

Final Report for
Highway IDEA Project 145

Prepared by:
Michael A. Mooney and Norman W. Facas
Colorado School of Mines

February 2013

TRANSPORTATION RESEARCH BOARD
OF THE NATIONAL ACADEMIES

Innovations Deserving Exploratory Analysis (IDEA) Programs
Managed by the Transportation Research Board

This IDEA project was funded by the NCHRP IDEA Program.

The TRB currently manages the following three IDEA programs:

- The NCHRP IDEA Program, which focuses on advances in the design, construction, and maintenance of highway systems, is funded by American Association of State Highway and Transportation Officials (AASHTO) as part of the National Cooperative Highway Research Program (NCHRP).
- The Safety IDEA Program currently focuses on innovative approaches for improving railroad safety or performance. The program is currently funded by the Federal Railroad Administration (FRA). The program was previously jointly funded by the Federal Motor Carrier Safety Administration (FMCSA) and the FRA.
- The Transit IDEA Program, which supports development and testing of innovative concepts and methods for advancing transit practice, is funded by the Federal Transit Administration (FTA) as part of the Transit Cooperative Research Program (TCRP).

Management of the three IDEA programs is coordinated to promote the development and testing of innovative concepts, methods, and technologies.

For information on the IDEA programs, check the IDEA website (www.trb.org/idea). For questions, contact the IDEA programs office by telephone at (202) 334-3310.

IDEA Programs
Transportation Research Board
500 Fifth Street, NW
Washington, DC 20001

Extraction of Layer Properties from Intelligent Compaction Data

IDEA Program Final Report

NCHRP-145

Prepared for the IDEA Program
Transportation Research Board
The National Academies

Michael A. Mooney and Norman W. Facas
Colorado School of Mines, Golden CO
February 2013

ACKNOWLEDGEMENTS

The authors are grateful to a number of companies for their input including Sakai, Case, Caterpillar, Trimble, and transportation agencies including the Minnesota and Colorado Departments of Transportation. The authors are grateful to the following individuals for their help throughout the project: Dr. Odon Musimbi, Dr. John Berger, Dr. Robert Rinehart, Dr. Judith Wang, Bernadette Kenneally, Aaron Neff, and Geoffrey Bee, all of Colorado School of Mines. Finally, the authors thank the NCHRP IDEA Program, including Program Manager Dr. Inam Jawed, for funding the study and providing assistance throughout the investigation.
.

TABLE OF CONTENTS

1 Introduction 2
2 IDEA Product 3
3 Concept and Innovation 4
4 Investigation 6
4.1 IC Data and Analysis 6
4.2 Forward Modeling 8
4.2.1 BE Analysis 8
4.2.2 FE Modeling 9
4.3 Parametric Studies 12
4.4 Inverse Analysis 14
4.5 Real Time Back-calculation 18
5 Plans for Implementation 21
6 Conclusions 22
References 23

EXECUTIVE SUMMARY

This reports details the findings of the National Cooperative Highway Research Program project 145 (NCHRP-145) titled "Extraction of Layer Properties from Intelligent Compaction Data." Vibratory roller-based measurement of soil and asphalt properties during and after compaction, an approach termed Continuous Compaction Control (CCC) or Intelligent Compaction (IC), has gained considerable momentum in the U.S. IC combines roller-based measurement of soil or asphalt properties with GPS-measured position to provide continuous assessment of stiffness over 100% of the production area. This constitutes a significant improvement over the coverage provided by spot test methods. One limitation of current IC technology is that the estimated soil or asphalt stiffness provided by vibratory smooth drum IC rollers (12-15 ton) is a composite measure of ground stiffness to a depth of 1.0-1.2 m. This is considerably greater than a 15-30 cm thick layer or lift of subgrade, subbase or base material, and thinner lifts of asphalt. While this composite measure of stiffness is informative, it does not provide a measure of layer elastic modulus/stiffness.

In this investigation, a methodology was developed to extract layer elastic modulus/stiffness from composite soil stiffness and GPS-based position provided by currently available vibratory IC rollers. The effort focused on soils but in principle is also applicable to asphalt. The developed methodology combines two key components that were advanced in this investigation, namely, forward modeling and inverse analysis Forward modeling efforts focused on finite element (FE) and boundary element method (BE) techniques to predict roller-measured composite stiffness values for ranges of layer elastic moduli and layer thickness expected in practice. Inverse analysis or back-calculation works in reverse and provides an estimate of individual layer elastic modulus using IC data. The back-calculation effort in this investigation focused on developing a real-time approach to modulus prediction and characterizing the uncertainty in estimated layer moduli based on measurement error and parameter sensitivity.

Both FE and BE forward modeling approaches were successful in explaining the relative influence of layer properties (layer modulus and layer thickness) on roller-measured composite soil stiffness. Forward model results matched relatively well with experimental data. Inverse analysis was pursued with a traditional gradient search approach that proved successful but time-intensive when using the FE or BE forward models. As a result, inverse analysis using FE or BE forward models cannot provide real-time back-calculation of layer moduli using current computing power. The development and use of a statistical regression forward model proved successful in capturing the essence of the FE and BE results and in enabling real-time inverse analysis to estimate layer modulus values.

The investigation demonstrated that layered elastic modulus can be estimated from IC data over a wide range of layered earthwork configurations (layer thickness and ratio of layer moduli). The ability to back-calculate layer modulus is influenced by measurement error (uncertainty) and parameter sensitivity. The uncertainty in back-calculated layer modulus increases as the top layer thickness decreases and/or as the ratio of a stiffer top layer modulus to bottom layer modulus increases. As an example, for commonly-used 15 cm thick lifts of aggregate base course over softer subgrade or subbase soil, the uncertainty in back-calculated base modulus can reach 50% as a direct result of typical IC data measurement error.

The methodology can be implemented via software algorithms that can be integrated into any commercially available IC software offered by roller manufacturers, consultants and third-party vendors, e.g., navigation system providers. IC software is used on-board the roller and/or on mobile and desktop computers. Therefore, the implementation of the methodology would be performed by the IC software companies. Alternatively, software algorithms could be employed independent of existing IC software. In this approach, the IC data (composite soil stiffness and GPS coordinates) from commercially-available software would be fed into a separate program that would provide layer moduli. The implementation of this latter approach could be performed by any interested party. The methodology generated is generic and can be applied to any currently-available proprietary measures of ground stiffness from vibratory rollers.

1 INTRODUCTION

The U.S. pavement community is making the important transition from quality control/quality assurance (QC/QA) via index property testing (e.g., density, moisture) to QC/QA via performance-based property testing (modulus, stiffness) to better align construction with mechanistic-empirical (M-E) design and to enable performance-based assessment of the constructed facility. As a result, vibratory roller-based measurement of soil properties during compaction, an approach termed Continuous Compaction Control (CCC) or Intelligent Compaction (IC), has gained considerable momentum in the U.S. IC combines roller-based measurement of soil properties with GPS-measured position and real-time graphical representation of data maps (as well as data storage) via an on-board computer (see Figure 1). IC is capable of providing continuous assessment of soil stiffness over 100% of the earthwork area, and constitutes a significant improvement over the coverage provided by spot test methods. Several studies have demonstrated the ability of vibratory smooth drum IC rollers (Figure 1) to assess soil stiffness, e.g. *(1), (2), (3*), as well as how roller-measured soil stiffness can be related to in-situ elastic modulus and how the stress field and data compares to that used in resilient modulus testing *(4), (5).* Both NCHRP and FHWA (pooled fund) studies have been completed and specifications for the implementation of IC have been developed *(6), (7).* Transportation agencies and State DOTs are now adopting IC specifications for pavement earthwork preparation.

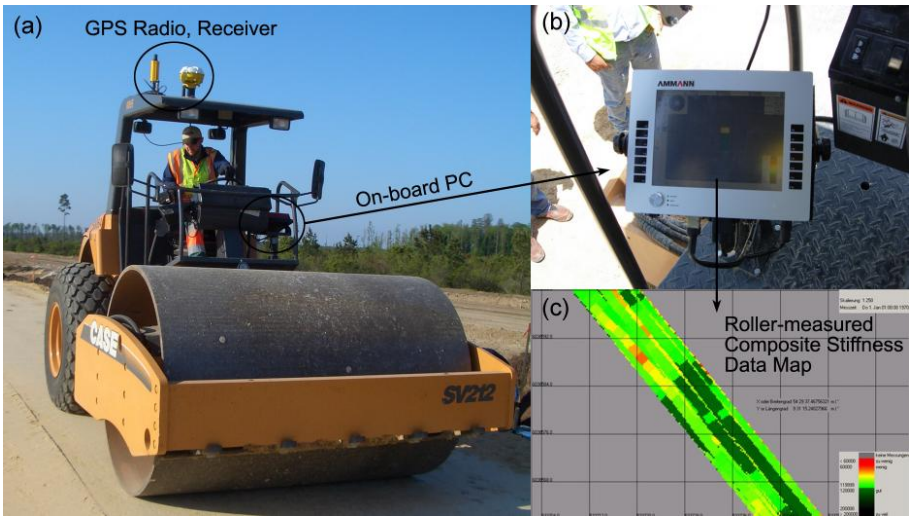

FIGURE 1: (a) IC roller with GPS and sensor data recorded by on-board computer; (b) close-up of on-board computer; and (c) roller-measured composite stiffness data map

One limitation of current IC technology is that the estimated soil stiffness provided by vibratory smooth drum IC rollers (12-15 ton) is a composite measure of ground stiffness to a depth of 1.0-1.2 m *(4).* This is considerably greater than a 15-30 cm thick lift/layer of placed subgrade, subbase or base material (see Figure 2). While this composite measure of soil stiffness is informative, it is more desirable to measure the stiffness/modulus of a 15-30 cm thick layer for two reasons. First, all U.S. transportation agencies currently perform earthwork QA on a per-lift basis. To be most effective in this system, the roller data should convey information to a similar depth, e.g., 15-30 cm (see Figure 2). A second reason to measure layer stiffness/modulus is to more directly align with M-E analysis and design, and therefore to performance-based QA. M-E design is predicated on the resilient elastic properties and thicknesses of base, subbase and subgrade layers (as well as the surface course). To this end, it is advantageous to provide independent measures of base, subbase and subgrade moduli. The goal of this research project, therefore, was to develop a methodology to extract layer-based or lift-based soil stiffness/modulus estimates from current IC roller data. The project focused on soil applications but is in principle also applicable to asphalt.

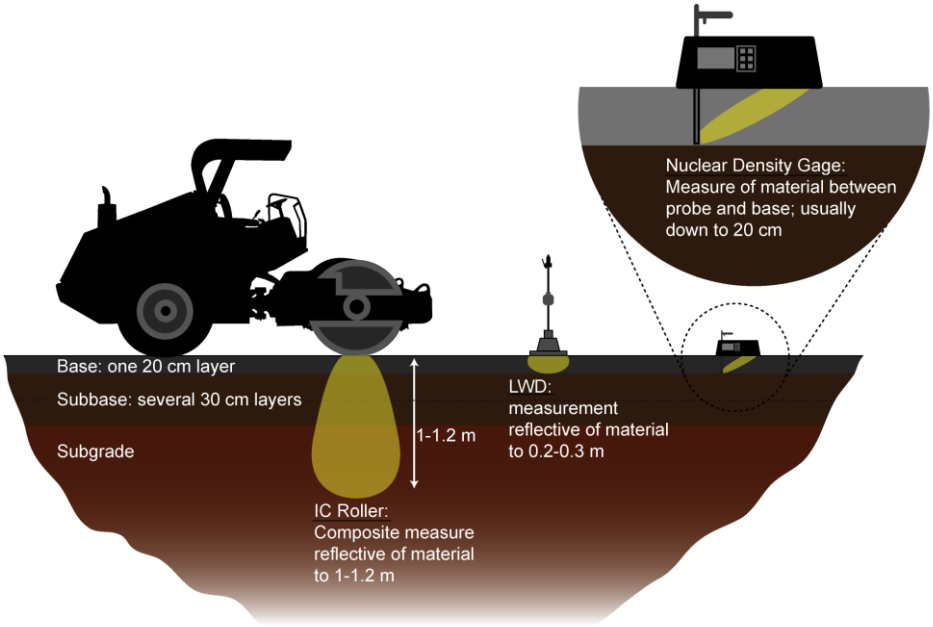

FIGURE 2: Measurement depths of IC roller and common field tests

2 IDEA PRODUCT

The product that will result from the knowledge developed during this investigation is a methodology that enables the extraction of layer stiffness/elastic modulus from currently available IC roller data (vibration-based stiffness and GPS position data). The resulting methodology can be explained using the illustration in Figure 3. All major manufacturers of roller compactors offer some form of IC technology for smooth drum vibratory rollers, i.e., the components in Figure 1. There are numerous different proprietary roller-based measures of soil stiffness in practice (e.g., see *(8)* for a review). Throughout this report, we designate k as a single roller-estimated value of composite soil stiffness. For each layer of pavement earthwork, e.g., subgrade, subbase, unbound base, an IC roller creates a spatial map of k data (Figure 3a). Technically, a spatial map of stiffness data can be designated by an array $k_i(x,y)$ that designates layer i and spatial coordinates x and y. Recall from the previous section that each measure of k reflects a composite stiffness to a depth of 1.0-1.2 m. Therefore, an IC data map created by measuring a base course layer is not providing the stiffness of the base layer alone; rather, it is a composite measure of the base, subbase and subgrade layered system. This is evident in practice by the correlation between stacked maps (Figure 3b). The product that will result from this investigation is illustrated in Figure 3c wherein the elastic modulus E of a single layer is extracted from a stack of IC data maps. This layer modulus data can then be used to directly assess the quality of the placed layer/lift.

The developed methodology can be implemented in practice through software algorithms. Such algorithms could be integrated directly into the IC equipment on-board an IC roller, within office software that analyzes IC data, or both. The methodology generated is generic and can be applied to any proprietary measures of ground stiffness. The methodology developed from this investigation will allow all transportation stakeholders (owners, consultants, contractors) to directly evaluate the elastic modulus of individual lifts or layers using vibratory IC roller data. This is currently not possible. The evaluation of individual lifts/layers is consistent with the philosophy of current QC/QA practice. In addition, the development of the described algorithm(s) aligns field measurement of modulus with the design process and performance-based QC/QA. For example, pavement design is based on the analysis of layered systems, each layer represented by strength, stiffness and permanent deformation characteristics. With regard to stiffness, the resilient modulus of each material is typically characterized via laboratory testing. These laboratory-determined values of resilient modulus are used to design the pavement system. By enabling the measurement of individual layer modulus in the field, one can assess the realized (constructed) elastic modulus relative to the designed-for resilient modulus. This moves the pavement community closer to performance-based QC/QA. This is not directly possible with current IC systems because there is no designed-for composite stiffness that currently available IC soil stiffness values can be compared to.

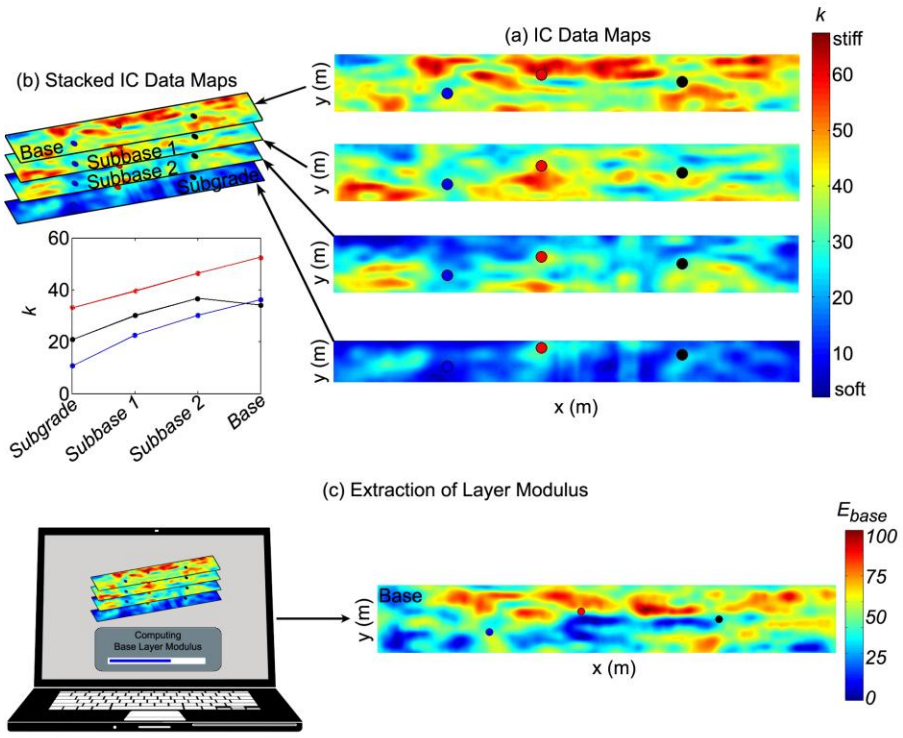

FIGURE 3: Schematic illustrating (a) individual IC roller-measured stiffness maps; (b) stacked IC data maps; and (c) the extraction of individual layer elastic modulus enabled by the developed methodology

3 CONCEPT AND INNOVATION

The developed methodology combines two key components that were advanced in this investigation, namely forward modeling and inverse analysis (Figure 4). Forward modeling involves the estimation or prediction of roller-measured composite stiffness values *k* for ranges of layer elastic moduli and layer thickness combinations expected in practice. Forward modeling can be physically-based, e.g., lumped-parameter, finite element, or boundary element modeling; it can be statistically-based; or it can be a combination of both. The state of the art in forward modeling of vibratory roller/ground interaction prior to this investigation has been based on discrete lumped parameter models, e.g., *(2), (9), (10), (11), (12), (13), (14)*, such as that shown in Figure 6. In the lumped parameter approach, the soil is modeled as a discrete mass-spring-dashpot element. This approach has been successful in 'lumping' all of the ground into a single object and in characterizing dynamic drum interaction. However, this approach is incapable of modeling individual earthwork layers and their contribution to IC roller response. Further, this approach cannot model the variable width contact problem between the drum and soil surface that is critical to correctly capturing layered soil response. In this investigation, continuum-based finite element (FE) analysis and boundary element (BE) analysis were employed to physically model individual layers and the nonlinear curved drum interaction with the ground surface (Figure 4a).

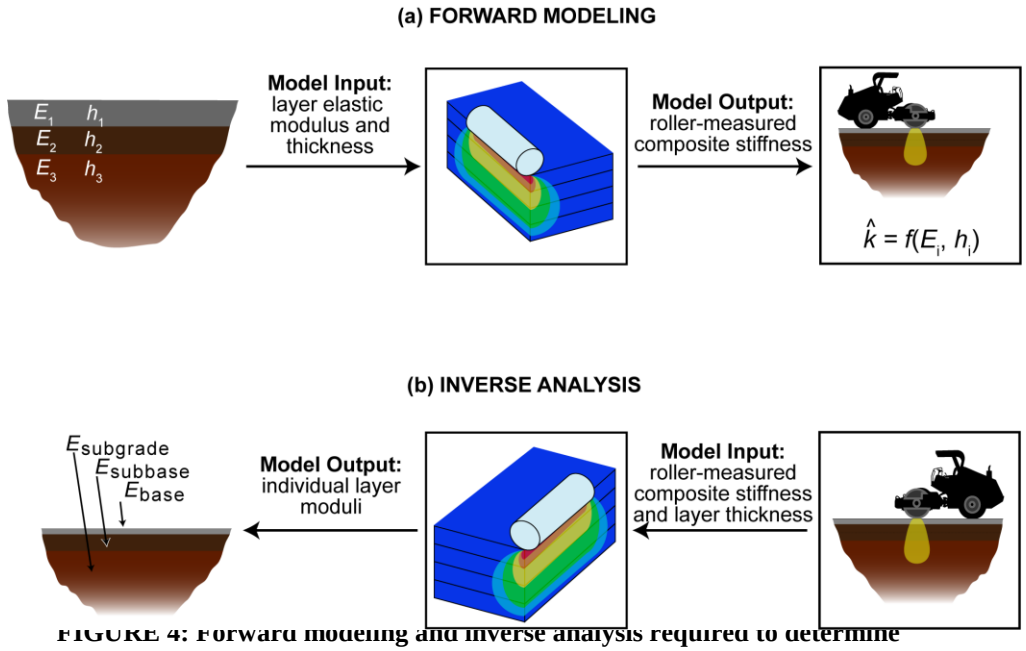

FIGURE 4: Forward modeling and inverse analysis required to determine layered elastic moduli from IC roller data

Inverse analysis works in reverse and provides an estimate of individual layer elastic modulus E_i using sets of IC data maps, i.e., k and layer thickness from stacked data sets (as shown in Figure 3). Inverse analysis, also called back-calculation, has a rich history but has not been applied to IC or similar moving machine data until this study. In this investigation, we employed inverse analysis to extract layer elastic modulus from IC roller measured data. The back-calculation of layer elastic modulus E_i for an n-layer system progression that follows a bottom-up construction process, beginning at the bottom layer (layer n in Figure 5). For pavement earthwork, layer n is the subgrade soil and is assumed to be at least 1-2 m thick and therefore behaves as a semi-infinite half-space. In this case, we can create a forward model (f_n) which relates the modulus of the bottom layer (E_n) to the roller measured stiffness (k_n) on the bottom layer. In this investigation we employed both finite element (FE) analysis and boundary element (BE) analysis to perform forward modeling. We assume that the soil is linear elastic, isotropic and homogeneous. We further assume that the Poisson's ratio is known and constant. To determine E_n from k_n we minimize the error between the measured k_n and the soil stiffness predicted by the forward model, i.e., $\hat{k}_n = f_n(E_n)$, where the hat implies forward model-predicted. The elastic modulus that minimizes this error function is deemed the best estimate of E_n.

For modulus back-calculation of the second layer from the bottom (layer n-1), the forward model f_{n-1} is a two layer model that is dependent on E_n, E_{n-1} and the thickness of the n-1 layer h_{n-1}. h_{n-1} can be determined with an accuracy of ±1-2 cm using RTK differential GPS position measurements from the roller operating on layers n and n-1. With h_{n-1} and E_n provided, f_{n-1} can be written in terms of the only unknown E_{n-1}. E_{n-1} is determined in an error minimizing fashion similar to how E_n was determined. In this case, the measured k_{n-1} is compared to the model-predicted $\hat{k}_{n-1}$. This process of modulus back-calculation can be continued to the next layer (i.e., n-2) and through to the top layer (i.e., layer 1). This method, summarized in Figure 5, is causal with respect to each layer. Thus, layer n only needs measurements on layer n to perform the back-calculation, layer n-1 only needs measurements on layer n and n-1, and so on to layer 1. Causality is an important property for the back-calculation as it allows elastic modulus to be computed on a per layer basis rather than having to wait until all of the layers are constructed, in which case it is too late to correct for any problem areas without significant cost.

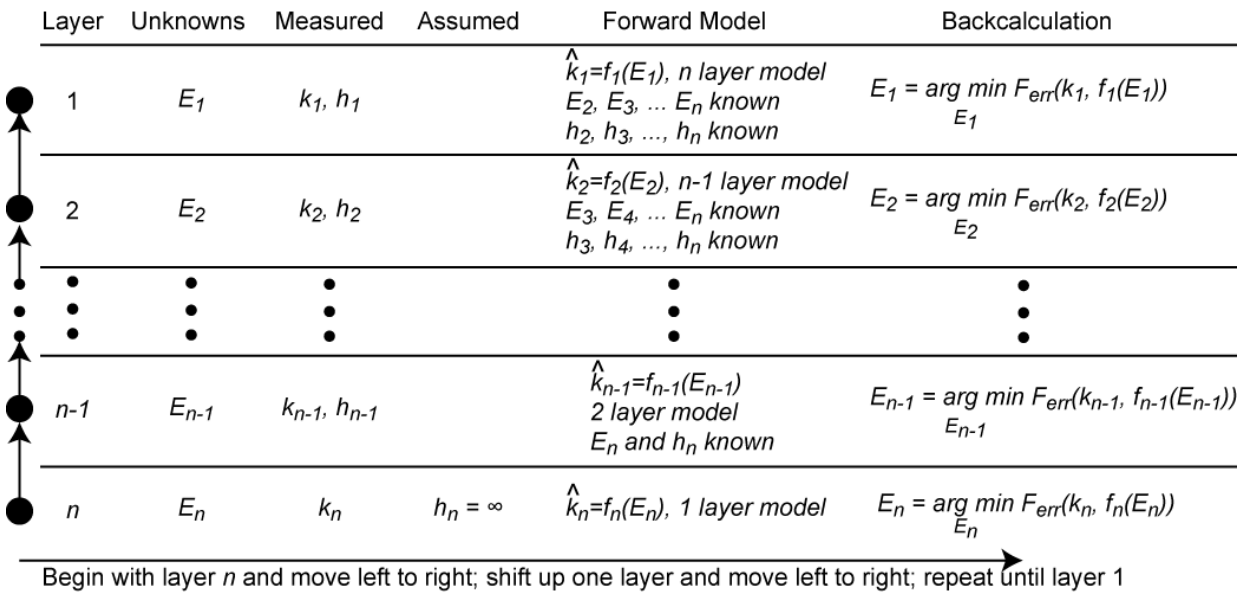

FIGURE 5: Back-calculation of an *n*-layer system

One limitation of back-calculation is that FE and BE analysis requires time. Ideally, the layer modulus should be calculated in real time onboard the IC roller as the composite stiffness and GPS data is collected. To accommodate real time inversion, we developed statistical models of the FE and BE analysis for a wide range of expected layered systems. The inverse analysis (back-calculation) therefore minimizes the difference between the measured and regression-modeled response to estimate layer modulus.

4 INVESTIGATION

The steps taken to develop the methodology included: (1) analysis of field data; (2) forward modeling development; (3) implementation of inverse analysis (back-calculation) and (4) regression efforts to enable real-time back-calculation. This section describes the research advanced in these areas.

4.1 IC DATA AND ANALYSIS

A basic level of IC roller fundamentals is required to follow the development of the methodology. Roller measured soil stiffness is derived from vertical force equilibrium of a vibrating drum (Figure 6). The force transmitted to the soil (contact force) is determined according to Equation (1):

$$F_c = F_e(t)\cos(\Omega t) + (m_f + m_d)g - m_d\ddot{z}_d - m_f\ddot{z}_f \quad (1)$$

where F_e(t) is the vertical (z direction) component of the excitation force produced by an eccentric mass configuration within the drum, Ω is the excitation frequency of the eccentric mass driven vibration, m_f and m_d are the frame and drum mass respectively, g is acceleration due to gravity, $\ddot{z}_f$ and $\ddot{z}_d$ are the accelerations of the frame and drum, respectively. By monitoring the position of the rotating eccentric mass and measuring the drum and frame accelerations, it is possible to estimate the force-deflection (F_c - z_d) behavior in real time. Figure 6 shows F_c - z_d response from a vibration cycle for continuous drum-soil contact (Figure 6b) and for partial loss of contact (Figure 6c). Partial loss of contact behavior is common at higher F_e levels and/or when operating on stiff soils. During loss of contact, F_c = 0. Two soil stiffness parameters used in current practice are illustrated in Figure 6. The soil stiffness parameter used by Ammann and Case (shown as k_b) is a secant stiffness from the point of zero deflection (under static loading) and static force through the point of maximum deflection *(2).* The soil stiffness parameter used by Bomag is based on a tangent stiffness from the loading portion of the curve (k_a). For the analysis and results presented here, we will employ k_b and generically refer to this composite soil stiffness as k. The findings presented here are applicable to each measure of composite stiffness.

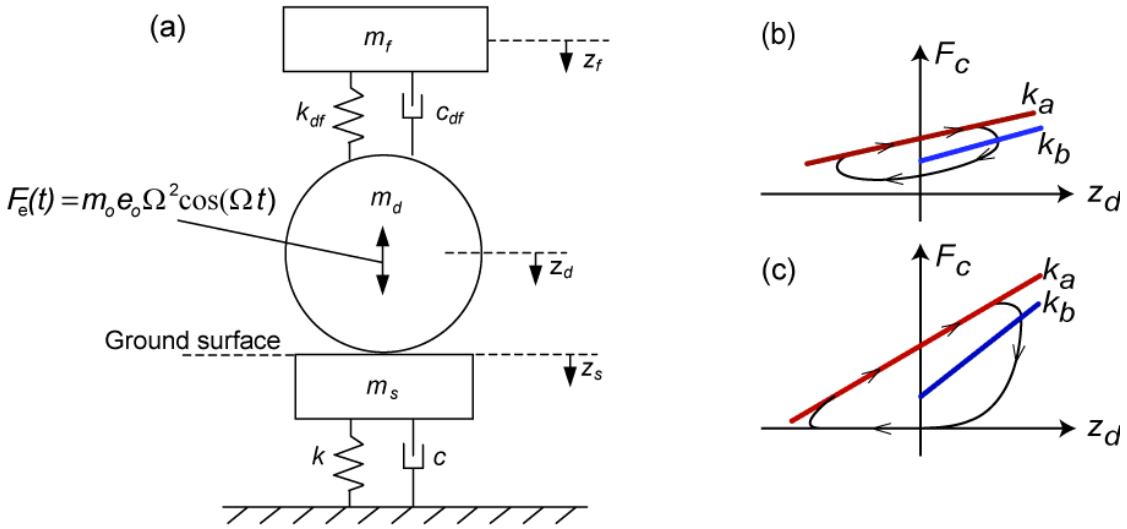

FIGURE 6: (a) Lumped parameter model of drum-soil interaction and (b-c) contact force vs. drum displacement response and composite soil stiffness measures for (b) contact mode and (c) partial loss of contact mode

The data used to calibrate/validate the forward finite element (FE) model was extracted from two test beds. The first test bed was a 30 m long lane of single drum width (2.1 m) of vertically homogenous silty sand (SM) subgrade soil. The soil was compacted using 10 roller passes of the instrumented Sakai SV 510D (Figure 9). The odd numbered passes were performed using forward direction roller travel low amplitude excitation force and 30 Hz excitation frequency. The measured F_s - z_d response (loops) shown in Figure 7 reveal the captured change in drum response and roller-measured soil stiffness k as a result of the compaction process. As a result of the compaction-induced increase in soil elastic modulus, the maximum z_d increases mildly, the maximum F_c increases significantly, and the ground stiffness (slope) increases appreciably. Partial loss of contact ensues during pass 7 and beyond. Forward modeling will need to capture this behavior.

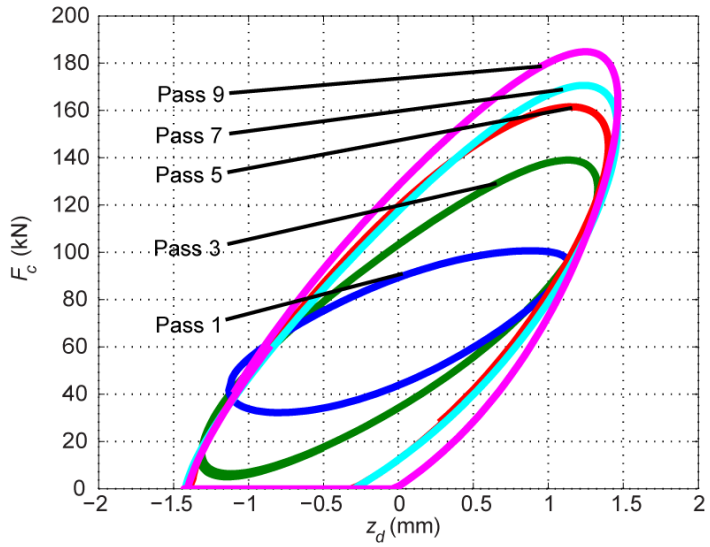

FIGURE 7: Field measured F_c - z_d loops from IC roller on vertically homogeneous subgrade soil

The second test bed was a layered system. On top of the granular subgrade, a 20 cm layer of stone base material was first placed and compacted. Then, a 30 cm layer of stone base material (for a total of 50 cm overlying layer) was placed and compacted. The F_c - z_d response from a low amplitude pass on each layer at the same spatial coordinates is shown in Figure 8. Independent density and stiffness testing revealed that each stone base layer reached similar levels of

compaction. As shown, the 20 cm and 50 cm thick layers of stiffer base course have a significant effect on the F_c - z_d response. Here, the F_c - z_d response reflects the composite two-layer system. F_c increases significantly with base course thickness, z_d increases slightly, and the composite stiffness k increases appreciably. Forward modeling must capture the composite nature of these responses.

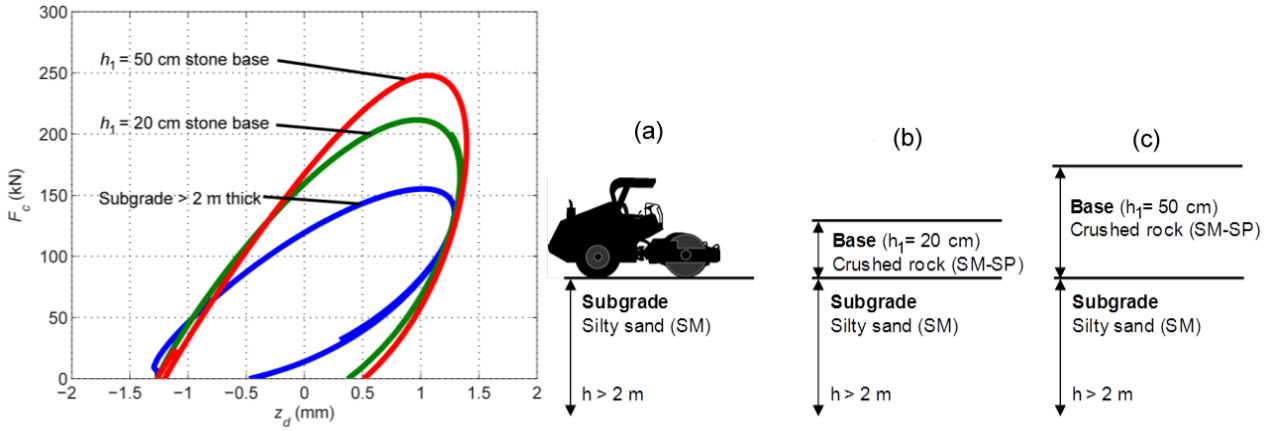

FIGURE 8: Field measured F_c - z_d loops from IC roller on vertically homogeneous subgrade soil and layered base over subgrade; (a) Subgrade; (b) 20 cm base over subgrade; (c) 50 cm base over subgrade

4.2 FORWARD MODELING

This investigation included the advancement of forward modeling in two areas, namely boundary element (BE) modeling and finite element (FE) modeling. We introduce these models here and refer the reader elsewhere for further detail, e.g. *(15).* The vibratory roller modeled in both BE and FE modeling is the Sakai SV 510D smooth drum (Figure 9). The model development is valid, however, for any vibratory roller as long as roller parameter values are known.

Parameter	Magnitude
Mass moment, $m_o e_o$	4.25 kg m
Vibration frequency, f ($\Omega/2\pi$)	30 Hz
Drum mass, m_d	4466 kg
Frame mass, m_f	2534 kg
Soil mass, m_s	0.3 m_d
Drum/frame stiffness, k_{df}	2.53 10^6 kg/s
Drum/frame damping, c_{df}	4000 kg/s
Soil stiffness, k	varies
Soil damping, c	varies

FIGURE 9: Sakai SV 510D smooth drum vibratory roller

4.2.1 Boundary Element Modeling

The BE method is a well-established tool used for stress and displacement analysis of layered continua *(16).* The advantage of BE analysis is that only the remote boundary of the material needs to be discretized; the resulting computation time is much shorter than required for FE analysis. The BE model used to simulate layered soil interaction with drum vibration is shown in Figure 10. A two-dimensional BE analysis code for the elasto-static solution of stress and displacement in anisotropic bi-materials was used to perform the analysis *(17).* This formulation is appropriate for plane-strain conditions and applicable to drum/soil modeling as Rinehart et al. *(18)* showed experimentally that plane-strain conditions exist beneath the center of the 2.1 m long roller drum. The layer materials are considered isotropic, and values of elastic modulus E and Poisson's ratio ν are summarized in Figure 10. The analysis performed here and in the FE modeling is limited to low drum vibration on fully compacted soil, a situation commonly used to assess as-built

stiffness of compacted soil. Under these conditions, the soil behaves elastically. To this end, the models do not capture the plastic deformation associated with compaction.

The BE approach does not explicitly model the drum; rather, a parabolic surface loading is applied to simulate the drum-soil contact force F_c. The amplitude $p(x)$ and the contact area $2a$ vary during each cycle of loading and loss of contact can be modeled, i.e., $2a = 0$. The contact force applied through parabolic loading is determined using a dynamic lumped parameter model (Figure 6) validated with extensive field data *(13)*. To this end, the approach is considered quasi-static. Both the applied force and the contact width over which the force is applied are determined through an iterative process until convergence. The BE analysis utilizes constant boundary elements, i.e., surface values of traction and displacement are assumed constant over each boundary element. Suitable mesh refinement studies were performed in advance of the numerical modeling; the final element length was 2 mm in the contact region.

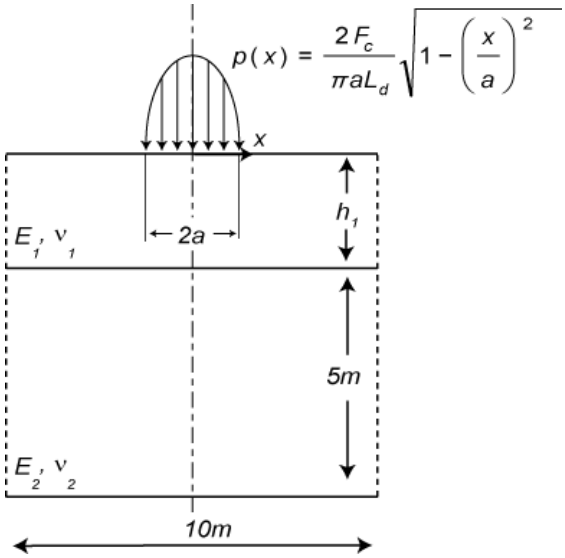

FIGURE 10: BE analysis to investigate influence of a two-layered system on roller measured *k*. The contact force F_c is applied as a parabolic surface traction $p(x)$; contact width $2a$ and F_c vary through iterative analysis until convergence (after *(15)*).

4.2.2 Finite Element Modeling

A 2D (plane strain) dynamic linear elastic FE model was developed to simulate and investigate vibratory drum interaction with layered soil. The key parameters of the model are illustrated and summarized in Figure 11. The 2D FE model employed vertical symmetry to optimize computational speed, and thus a one-half model was created. This model used two different types of elements. In the region directly under the drum, 100 mm x 100 mm square elements were used over a 2m x 2m area. In the far field, infinite elements were used to absorb wave energy and prevent unnatural reflections. In addition to the geometric damping that occurs naturally in the model, Rayleigh damping was introduced to simulate material damping in the soil. The damping matrix [C] is defined by two parameters α and β by Equation (2):

$$[C] = \alpha[M] + \beta[K] \tag{2}$$

where [M] is the mass matrix and [K] is the stiffness matrix. Rayleigh damping is a standard method of damping model in time-domain FE. The limitation of this approach, however, is that parameters α and β lack a physical meaning and therefore are arbitrarily assigned to fit experimental data.

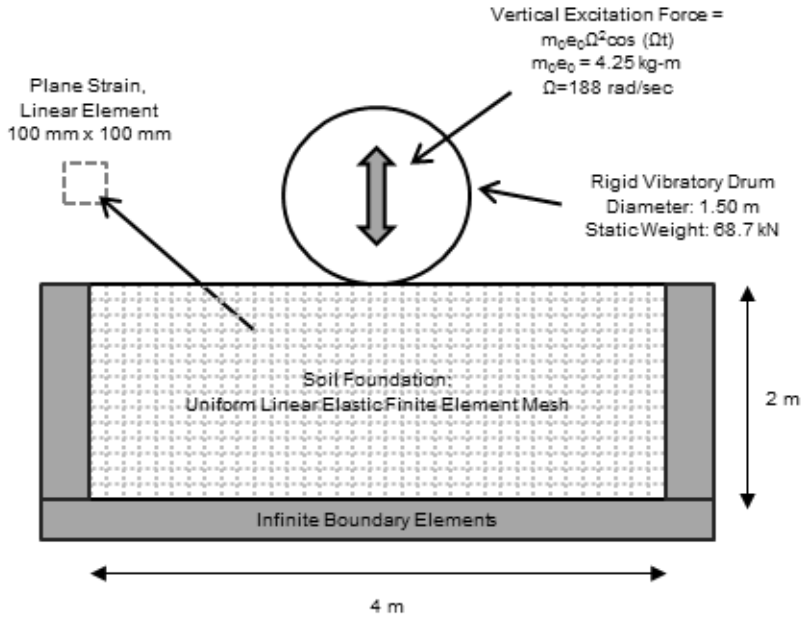

FIGURE 11: 2D FE model with infinite elements

The FE simulations were fit to the experimental data from the vertically homogeneous test bed 1 (Figure 7) using $\alpha = 25$, $\beta = 0.0002$, mass density $\rho = 2000$ kg/m^3, and E values shown in Figure 12. The α and β parameters were kept constant for all of the FE matching simulations for model simplification. Admittedly, the fitted density should increase from pass to pass; however, the change in density is typically only 10-15% from initial to final states; this difference has little influence on simulated response. Based on the resulting fits in Figure 12, constant α, β and ρ parameters are a reasonable assumption. The FE results appear very similar to the measured data. For the partial loss of contact response, the FE results begin to diverge from the measured results, where the FE peak forces are lower than those estimated from measured data. Lightweight deflectometer (LWD) testing was performed to independently assess the elastic modulus. The average of two LWD tests is provided for each fit in Figure 12. The trend of E_{lwd} vs. FE model E is shown in Figure 12f. Finally, the FE-simulated F_s - z_d response produced k values that very closely matched field-measured values (see Table 1).

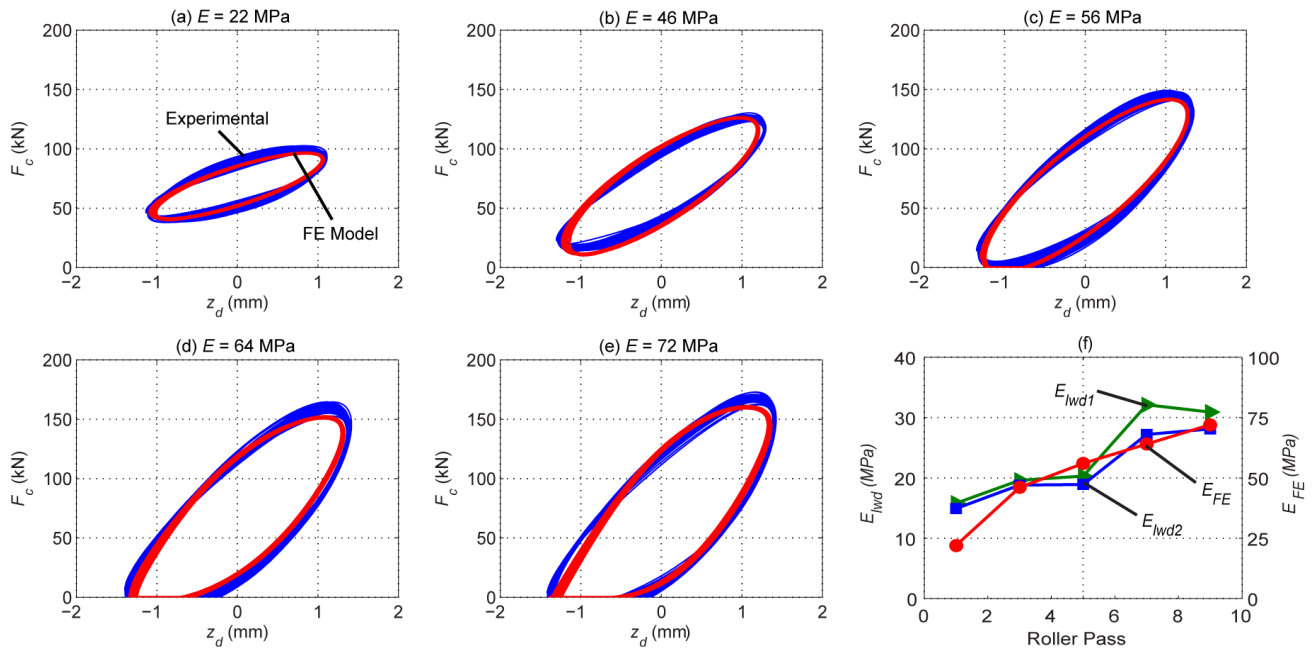

FIGURE 12: Comparisons between field-measured IC data and fitted FE results using $\alpha = 25$, $\beta = 0.0002$, $\rho = 2000$ kg/m^3, and E provided in each caption; (f) E_{lwd} from LWD testing are shown.

TABLE 1: Comparison of subgrade k from measured data and FE results

Pass	k (measured) (MN/m)	k (from FE) (MN/m)	Error (%)
1	21.2	20.9	-1.4
3	38.4	39.1	1.8
5	46.8	47.3	1.1
7	53.0	53.0	0.0
9	56.8	57.0	0.4

The 2D FE simulations on layered earthwork were next fitted to the experimental results from Figure 8. The FE-simulated and experimental results are plotted in Figure 13. For each simulation, $\alpha = 25$, $\beta = 0.0002$, and $\rho = 2000$ kg/m^3, similar to the previous analysis. Resulting values of $E_{subgrade}$ and E_{base} were 70 MPa and 210 MPa, respectively. The difference between simulated and field-measured k are shown in Table 3. The difference is high for the two-layer systems because the computation for k is quite sensitive to when the peak drum deflection occurs. For the FE results, the peak deflections occurred at lower contact force amplitudes, resulting in a decreased k. Generally the fits are somewhat similar; however, the results for high levels of loss of contact still need improvement. It may also be possible that the α and β should be different for the stone base material to achieve better fits. However, with α and β as arbitrary fitting parameters, such an approach would result in many unknowns that could not reliably be extended to other layered situations.

TABLE 2: Fit parameters for layered test bed

Layer	α	β	ρ (kg/m^3)	E (MPa)
Subgrade	25	0.002	2000	70
Stone Base 0.2m	25	0.002	2000	210
Stone Base 0.5m	25	0.002	2000	210

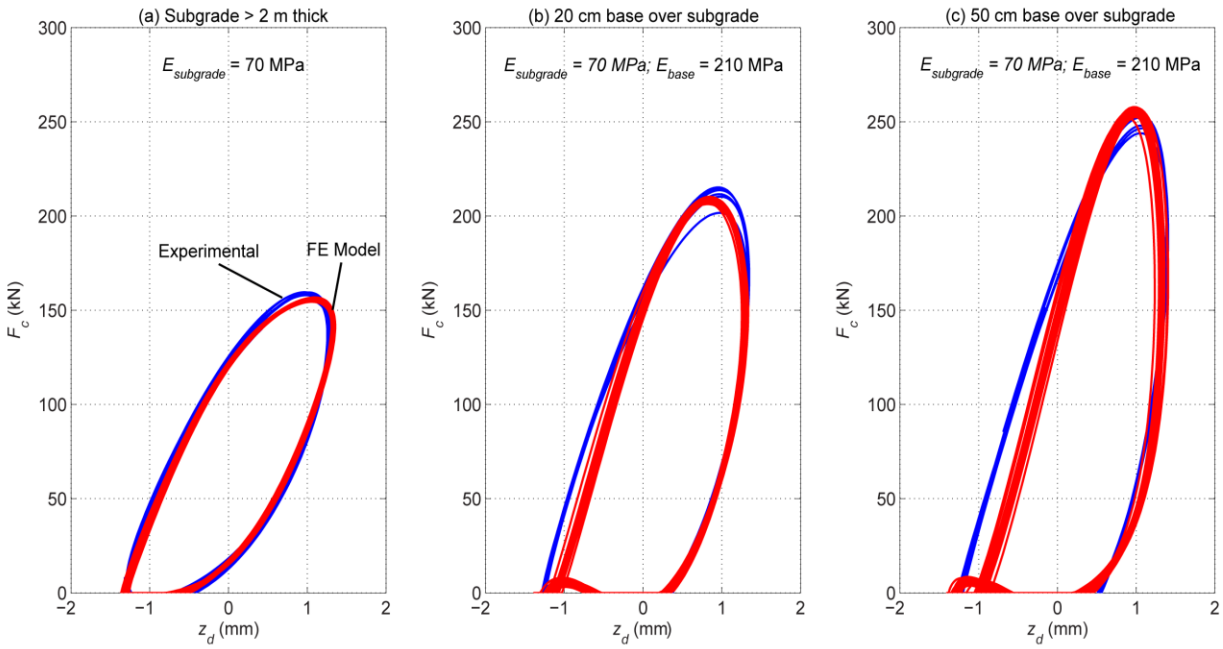

FIGURE 13: Comparisons between field-measured IC data and fitted FE results for base over subgrade earthwork (α = 25, β = 0.0002, ρ = 2000 kg/m^3, and fitted *E* provided in each caption).

TABLE 3: Comparison of *k* from measured data and FE results for two-layer system

Pass	*k* measured (MN/m)	*k* FE (MN/m)	Error (%)
Subgrade	52.3	54.9	5.0
Stone Base 20 cm	72	60.9	-15.4
Stone Base 50 cm	88.1	72.6	-17.6

4.3 PARAMETRIC STUDIES

To better characterize drum response anticipated across a range of layered earthwork situations, three parameter studies were performed with the FE model. Parametric study results from BE analysis are presented in Section 4.4. In each of the three studies, α, β and ρ values remained constant (α = 25, β = 0.0002, ρ = 2000 kg/m^3). The first parametric study varied *E* for a vertically homogenous soil condition. This would simulate IC data on a compacted subgrade or subbase material that has a thickness greater than 1.2 m. Here, *E* is varied from 10 to 100 MPa as a typical range of subgrade modulus. As observed in Figure 14, the simulated *k* varies linearly with *E* until approximately 55 MPa where partial loss of contact ensues. Thereafter, *k* increases in nonlinearly with *E*.

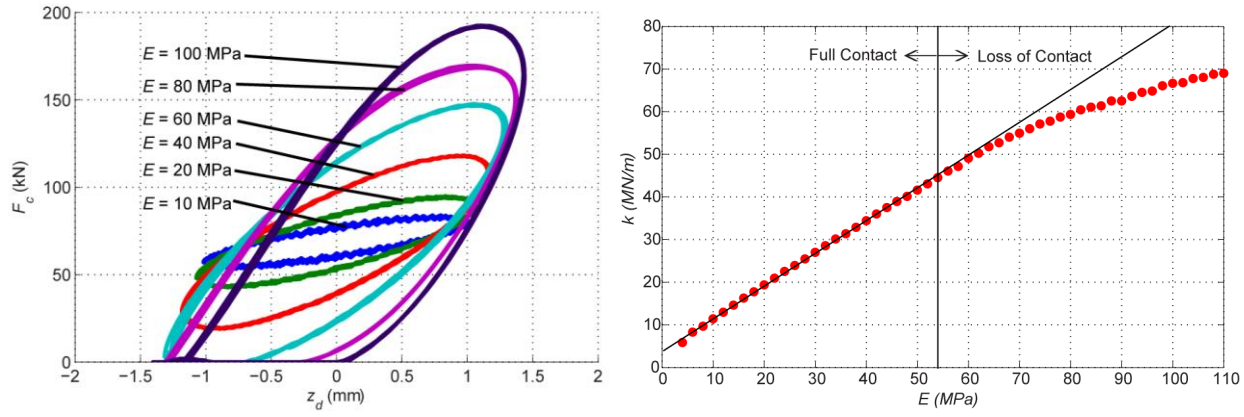

FIGURE 14: FE-simulated F_c - z_d and k on a vertically-homogeneous elastic half space

A second parametric study was performed on a two-layer system to examine the influence of the ratio E_1/E_2 on IC response, where E_1 is the modulus of the top layer and E_2 the underlying layer. The top layer thickness was fixed at h_1 = 0.8 m and E_2 = 50 MPa. The results from the FE can be seen in Figure 15. At high modulus ratios, the F_c - z_d loops become very steep. The resulting k values increases with E_1/E_2 as would be expected. Recall that the layered FE model was calibrated for E_1/E_2 = 3 and h_1 = 20 cm and 50 cm. The FE-simulated results in Figure 15 admittedly extend well beyond these calibrated ranges where there is no experimental data for verification.

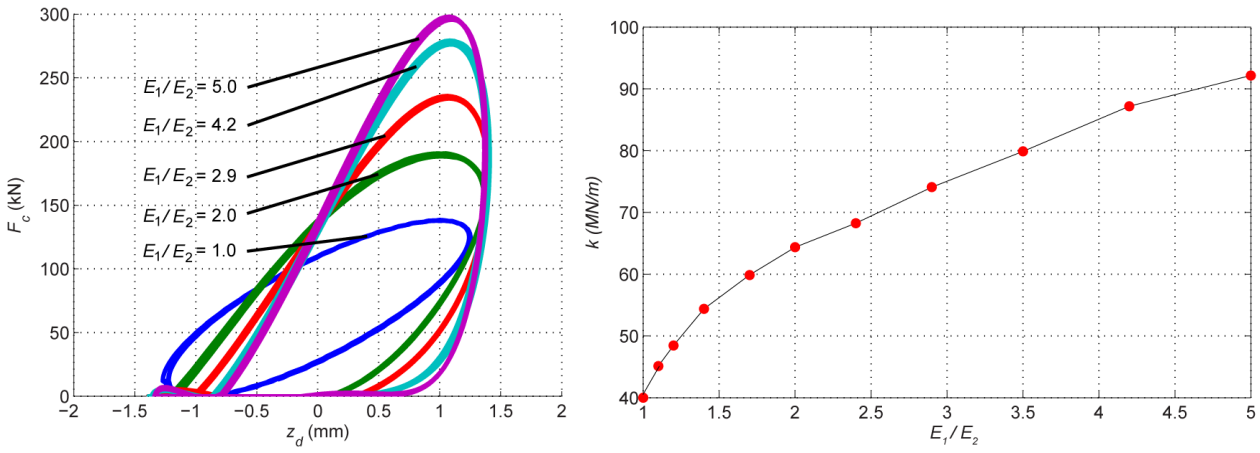

FIGURE 15: FE-simulated F_c - z_d and k on a h_1 = 0.8 m thick layer overlying a 50 MPa elastic half space as the overlying layer E_1 is varied from 50 to 250 MPa.

A third parametric study was performed to examine the effect of top layer thickness h_1 on IC data (Figure 16). h_1 was varied from 0 (homogeneous half space) to 0.8 m for E_2 = 50 MPa and E_1 = 100 MPa. The resulting k values increase with h_1 and trend towards k = 68 MN/m represented by the horizontal line. The k = 68 MN/m is consistent with a homogeneous elastic half space of E = 100 MPa.

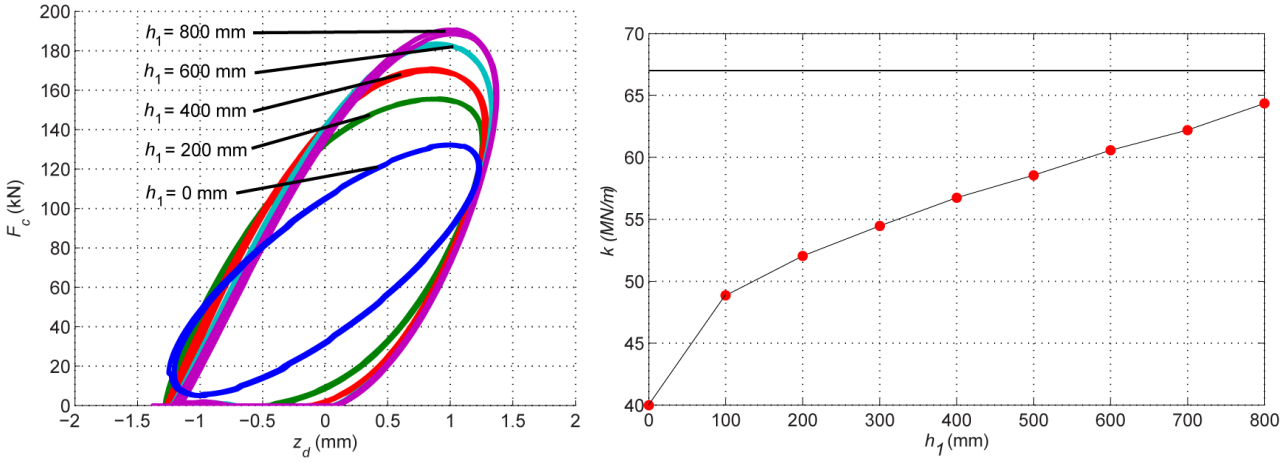

FIGURE 16: FE-simulated F_c - z_d and k for two-layer system (E_2 = 50 MPa, E_1 = 100 MPa) where h_1 is varied from 0 to 0.8 m

BE forward model results are presented in Section 4.4 within the context of inverse analysis. However, before leaving the FE model results, FE and BE model results are compared. For illustrative purposes, results from FE and BE simulations of a two layer earthwork system with h_1 = 30 cm are presented in Figure 17. The results are presented as contour plots of k as a function of E_1 and E_2. While the general trends and magnitudes are similar, the values of k at each E_1 and E_2 combination are different. This is likely a result of the fully dynamic FE simulations vs. the pseudo-static BE simulations. The contours for the BE analysis are monotonic functions, i.e., for fixed k, E_1 maps to only one E_2 and the order of E_1 is preserved in the corresponding E_2. However the contours for the FE simulations are not monotonic functions, i.e., for fixed k any E_1 does not map to only one E_2.

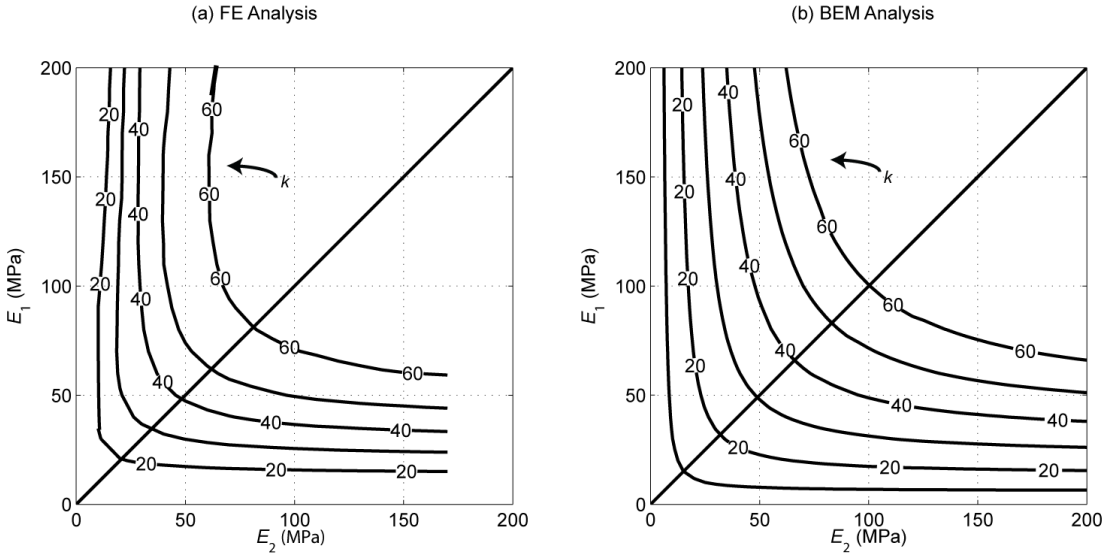

FIGURE 17: Comparison of simulated k values from (a) FE analysis and (b) BE analysis for a two-layer system with h_1 = 30 cm.

4.4 INVERSE ANALYSIS

Here we illustrate the back-calculation of layer modulus for a two-layer system (Figure 18). We employ the BE forward model within this inversion process. In practice, either BE or FE results can be used. Recall that three key parameters dictate the roller response for a two layer system: the top layer elastic modulus (E_1), the bottom layer elastic modulus

(E_2), and the thickness of the top layer (h_1), which is determined from GPS measurements. E_2 is known because it was determined from inversion of IC results from layer 2 on down (described in Section 3).

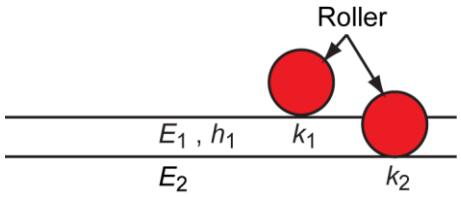

FIGURE 18: Two-layer system used for inverse analysis.

The required nature of the back-calculation approach was determined through investigation of the roller-layered soil response. The forward model-predicted k was simulated using the pseudo-static BE analysis over a wide range of E_1, E_2 and h_1 consistent with what is observed in practice. The k values vs. E_1 and E_2 are plotted for h_1 =15, 30 and 50 cm in Figure 19. The BE results in Figure 19 are physically intuitive, e.g., k increases with increasing E_1 and E_2. All of the contours exhibit monotonically decreasing k from left to right as E_2 decreases. Figure 19 conveys the uniqueness of k in that there is only one E_1 - E_2 combination that produces a measured k for a given h_1. Additionally, as h_1 increases, a lower E_2 is needed to maintain the same k_1 for fixed E_1 (for $E_1 > E_2$). This implies that as h_1 increases, the top layer has a larger influence on k_1.

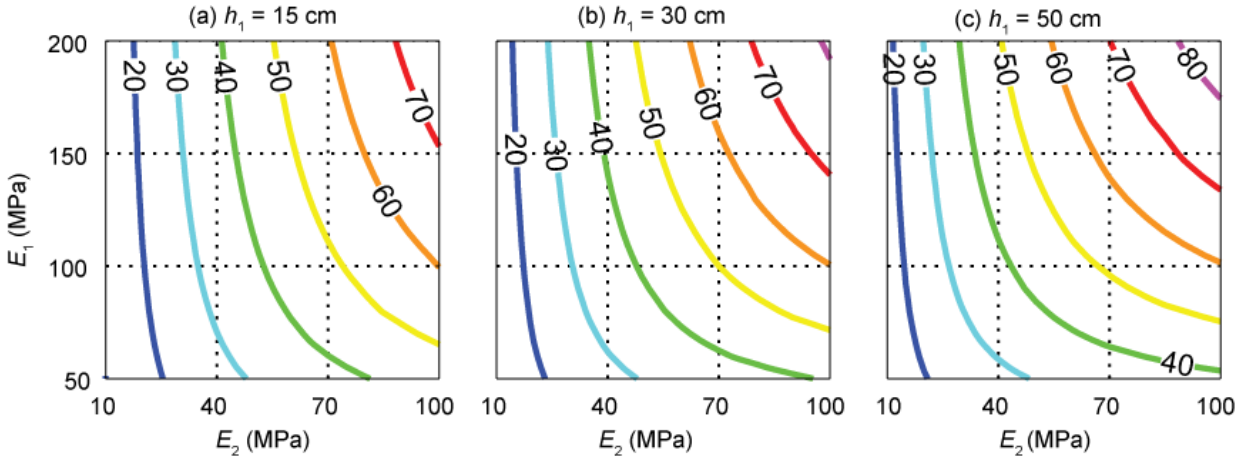

FIGURE 19: Simulated *k* values (MN/m) from BE modeling for (a) h_1 = 15 cm (b) h_1 =30 cm and (c) h_1 = 50 cm

The gradients or partial derivatives of the Figure 19 contours reflect the relative influence of each parameter on k. More specifically, the gradients $\partial k/\partial E_1$, $\partial k/\partial E_2$ and $\partial k/\partial h$ reflect the *sensitivity* of k to E_1, E_2 and h_1. These sensitivities were numerically estimated from the BE analysis results using the central difference method and forward/backward differences on the edges of the data set. They are presented in Figure 20 in E_1 vs. E_2 space for h_1 = 15, 30 and 50 cm. The non-zero sensitivities throughout Figure 20 indicate that E_1 and E_2 always influence k to some degree for the ranges of E_1, E_2 and h_1 evaluated. For these values typically observed in earthwork practice, the higher values of $\partial k/\partial E_2$ in Figure 20 clearly show that k is more sensitive to the underlying layer modulus (E_2) than the top layer (E_1) for most earthwork conditions. These results are critical to successful back-calculation of layered elastic modulus from roller measured k. Selected additional findings are highlighted using the following numerical notations in Figure 20: (1) when the top layer is much stiffer than the underlying layer (e.g., E_1/E_2 = 6), k is very weakly affected by the top layer (E_1); (2) as E_1/E_2 increases, k becomes less sensitive to the top layer (E_1); (3) as E_1/E_2 increases, k becomes more sensitive to the underlying layer (E_2); (4) as h_1 increases, k is more influenced by E_1 and less influenced by E_2.

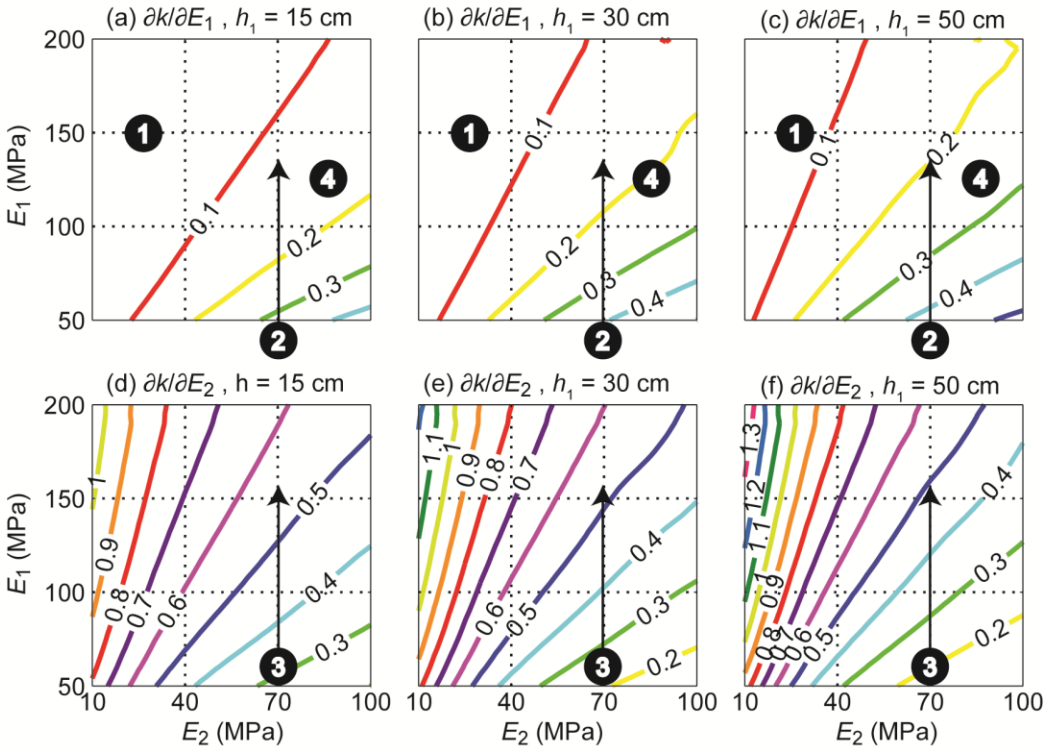

FIGURE 20: Sensitivity of roller-measured *k* (MN/m) to layer moduli for h_1 = 15 cm (left column), h_1 = 30 cm (middle column) and h_1 = 50 cm (right column).

Figure 21 presents the BE-determined k vs. E_1 for various values of E_2 and h_1. The relationships are monotonically increasing functions, implying that the inversion should be unique, i.e., for each k there exists exactly one value of E_1 for given E_2 and h_1. Thus, there are no local minima or maxima when performing the inversion. Based on these findings, simpler minimization algorithms such as a root finding algorithm can be used. More complex minimization techniques such as genetic algorithms *(19)* are not required.

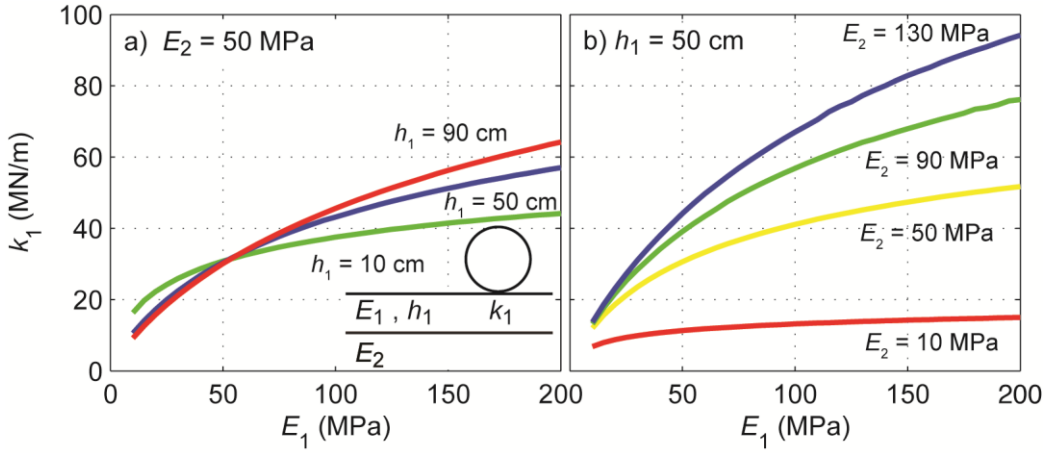

FIGURE 21: BE model-simulated *k* vs E_1 for a two-layer system for: (a) variable h_1, (b) variable E_2

The secant method was used to back-calculate E_1 by finding the zero of the difference between the measured and model-predicted stiffness given by the error function F_{err} (Equation 3):

$$F_{err}(E_1) = k - f_1(E_1) \tag{3}$$

Recall that f_1 is only a function of E_1 since E_2 and h_1 are assumed known before performing the back-calculation. Per the secant method, E_1 is determined by iteration via Equation (4):

$$[E_1]_{i+1} = [E_1]_i - \frac{[E_1]_i - [E_1]_{i-1}}{F_{err}([E_1]_i) - F_{err}([E_1]_{i-1})} F_{err}([E_1]_i) \quad (4)$$

where i is an integer for the current iteration and $[E_1]_i$ is the value of E_1 after the i^{th} iteration. To use the secant method, an initial estimate of both $[E_1]_0$ and $[E_1]_1$ is required; these estimates should not be equal. For the analysis here, $[E_1]_0$ was determined via the assumption that the soil is a homogeneous half-space; $[E_1]_1$ was estimated as a slight offset from $[E_1]_0$. The iterations were continued until the per-step change in E_1 was 0.001 MPa or less. The inversion approach was performed for a range of E_2 (20, 40 and 80 MPa), E_1 (40, 80, and 160 MPa) and h_1 (10, 50, and 90 cm). Each back-calculated E_1 matched the input E_1 to within 0.006% and was thus successful.

The ability to back-calculate E_1 is significantly influenced by the sensitivities presented in Figure 6 and the error or uncertainty in IC roller measurements. Here, the term $\varepsilon_k^{E_1}$ is defined as the percent error in back-calculated E_1 due to a unit percent error in k. Because it is determined from roller measurements, k will include measurement error. Therefore, $\varepsilon_k^{E_1}$ conveys the propagation or gain in error as a result of k measurement error and model sensitivity. $\varepsilon_k^{E_1}$ is determined from the inverse of the forward model sensitivities normalized by E_1 and k as shown in Equation (5). Similar formulae exist for $\varepsilon_{E_2}^{E_1}$ and $\varepsilon_{h_1}^{E_1}$ that convey the percent error in E_1 due to a unit percent error in E_2 and h_1, respectively. The error in back-calculated E_1 is presented graphically in Figure 22 for the ranges of E_1, E_2 and h_1 investigated. Values of $\varepsilon_k^{E_1}$, $\varepsilon_{E_2}^{E_1}$ and $\varepsilon_{h_1}^{E_1}$ are greatest where the sensitivities are the lowest, and in general, the error in E_1 will almost always be magnified, i.e., $\varepsilon^{E_1} > 1$.

$$\varepsilon_k^{E_1} = \frac{\partial E_1}{\partial k} \frac{k}{E_1} \quad (5)$$

The recently completed NCHRP 21-09 study on intelligent soil compaction revealed that typical percent uncertainties (coefficients of variation) in k, E_2 and h_1 were found to be 5%, 10%, and 10-15%, respectively, based on multi-site testing with different rollers and unbound materials *(7).* These input parameter errors influence the uncertainty in back-calculated E_1 via the factors $\varepsilon_{k_s}^{E_1}$, $\varepsilon_{E_2}^{E_1}$ and $\varepsilon_{h_1}^{E_1}$, and illustrate the difficulty in precise estimates of E_1 via back-calculation. For example, per Figure 22a, $\varepsilon_k^{E_1}$ = 5-7 for h_1 = 15 cm stiff base over a soft subgrade (E_1 > 150 MPa, E_2 < 30, E_1/E_2 > 5); the resulting uncertainty in E_1 is significant, i.e., 5% (5-7) = 35-45%. The uncertainty in estimated E_1 decreases for increasing h_1 and decreasing E_1/E_2. Similarly, 10% uncertainty in E_2 translates into 10-55% error in E_1 depending on the E_1, E_2, h_1 conditions. Finally, a 10-15% uncertainty in h_1 resulting from GPS error translates into a 0-20% error in E_1. As a related note, lift thickness varies spatially due to the imprecise nature of earthwork construction. If this were not considered in back-calculation, additional error would be introduced. However, continuous GPS measurements allows for spatial characterization of layer thickness and incorporation into back-calculation.

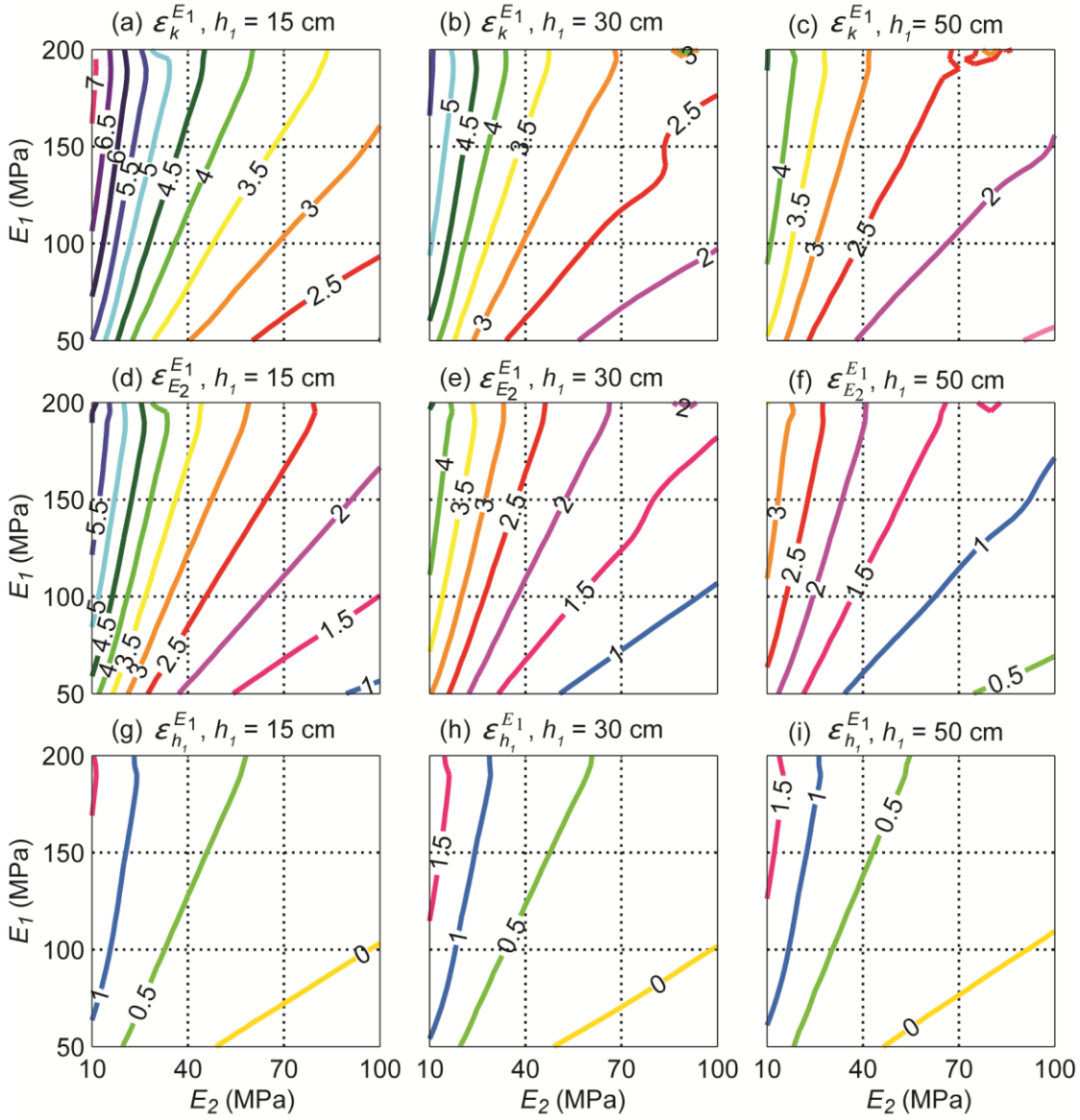

FIGURE 22: Error in back-calculation of E_1 given a unity percentage uncertainty in k (top row), E_2 (middle row) and h_1 (bottom row) as a function of E_2.

The results in Figure 22 illustrate that as h_1 decreases and E_1/E_2 increases, as is characteristic of thin aggregate base layers overlying subbase or subgrade, the back-calculation of top layer E_1 becomes increasingly difficult and prone to considerable uncertainty. As with all test results, measurement uncertainty should be accounted for statistically. To achieve a certain level of confidence that the back-calculated layer moduli will meet or exceed a desired or *target* moduli (where the target value is tied to design), the probability distribution of the measured (back-calculated) moduli is considered (e.g., mean and variance for a normal distribution). Accordingly, high levels of uncertainty in the data will increase the mean back-calculated moduli required to satisfy the desired level of confidence.

4.5 REAL TIME BACK-CALCULATION

The motivation for this study is the *real-time* estimation of layer modulus, i.e., as the IC roller data is streaming into the on-board system. With field sampling rates of 10 Hz (approx. spatial resolution of 10 cm), each inversion must be performed in approximately 0.1 s. However, the back-calculation approach described thus far is too time intensive. Each inversion required 5-15 iterations and within each iteration, forward modeling must be performed. Each BE or FE analysis required 30 s or more. Each back-calculation therefore required 2.5-7.5 minutes. To increase the efficiency of the

back-calculation, a regression modeling approach was pursued to represent the forward model in the back-calculation process. Typically, rather than simulating the forward model, direct inverse models are created through regression models. However, better results can be achieved by simulating the forward model *(20).*

Three empirically based regression models were created from a training data set generated using the BE results. The three models include: (1) a database with local interpolation, (2) a polynomial fit, and (3) an artificial neural network (ANN). ANNs have been used for back-calculation problems either to simulate the forward model results or to create a direct inverse model, e.g., *(20), (21);* see *(22)* for additional usage. However the other proposed regression models offer great promise for this problem particularly when simulating the forward model. A database of results using interpolation relies on an array of BE results from pre-defined parameter fields (e.g., Table 1). Local interpolation can be performed to predict results between entries. When the database has gridded data, as is the case here, efficient local interpolation algorithms such as cubic interpolation can be applied. The advantage of the database and interpolation model is that it is simple to create and understand. The main disadvantage is that it requires storage of the training set and requires a dense training set to get good results.

The model used for the polynomial fit is given by Equation (6):

$$k = \sum_{i=0}^{p_{max}} \sum_{j=0}^{p_{max}-i} \sum_{k=0}^{p_{max}-i-j} c_{ijk} E_1^i E_2^j h_1^k \qquad (6)$$

where c_{ijk} are the fitted model constants and p_{max} is the maximum allowed power. To determine the model constants, a least square approach was used on the BE based training data. The advantage of the polynomial fit approach is that a physical meaning can be extracted from the model. The disadvantage is that some physical knowledge of the system is needed to develop robust polynomial models.

The final empirical approach that was examined is an artificial neural network (ANN). An ANN is a connection of perceptrons. A perceptron takes a weighted sum of it inputs and applies a sigmoid function to produce a single output. The ANN is made up of the input layer, the hidden layer and the output layer. The input layer takes in the parameters. These inputs are each connected to each perceptron in the hidden layer (for a fully connected ANN). There can exist multiple hidden layers where each consecutive hidden layer is connected to the previous layer. The last hidden layer is connected to the output layer. To enable regression, the output layer does not use a sigmoid function for its perceptron. The structure of the ANN is given by the number of perceptrons in each layer starting with the hidden layer, e.g., a 35-1 ANN would have 35 perceptrons in the hidden layer and 1 perceptron in the output layer. To determine the weights in the ANN (i.e., the weight for each input of each perceptron), a back-propagation algorithm is used, e.g., *(23)*. The back-propagation algorithm is an iterative process that minimizes the error between the ANN outputs and the training set outputs.

The three models: (1) database with local tri-cubic interpolation (LTC), (2) 9th order polynomial model (Poly), and (3) a 35-1 ANN with a hyperbolic tangent sigmoid transfer function, were fit to BE forward model results. Each model was trained with a ~12.5% subset of the original data set and then evaluated against the balance of the data set. Data simulated using each of the models and the test data set are plotted for three values of h_1 in Figure 23. Each model produced similar results and matches well with the BE results. The error (absolute percent difference) in k between the BE model and the regression models over the entire simulation set is summarized in Table 4. The ANN yielded the highest errors at 5% whereas the LTC and 9th order polynomial models yielded errors around 2%. For 99% of the data, error was less than 1% for all regression models. Generally speaking, each model was able to simulate the BE model results with acceptable error.

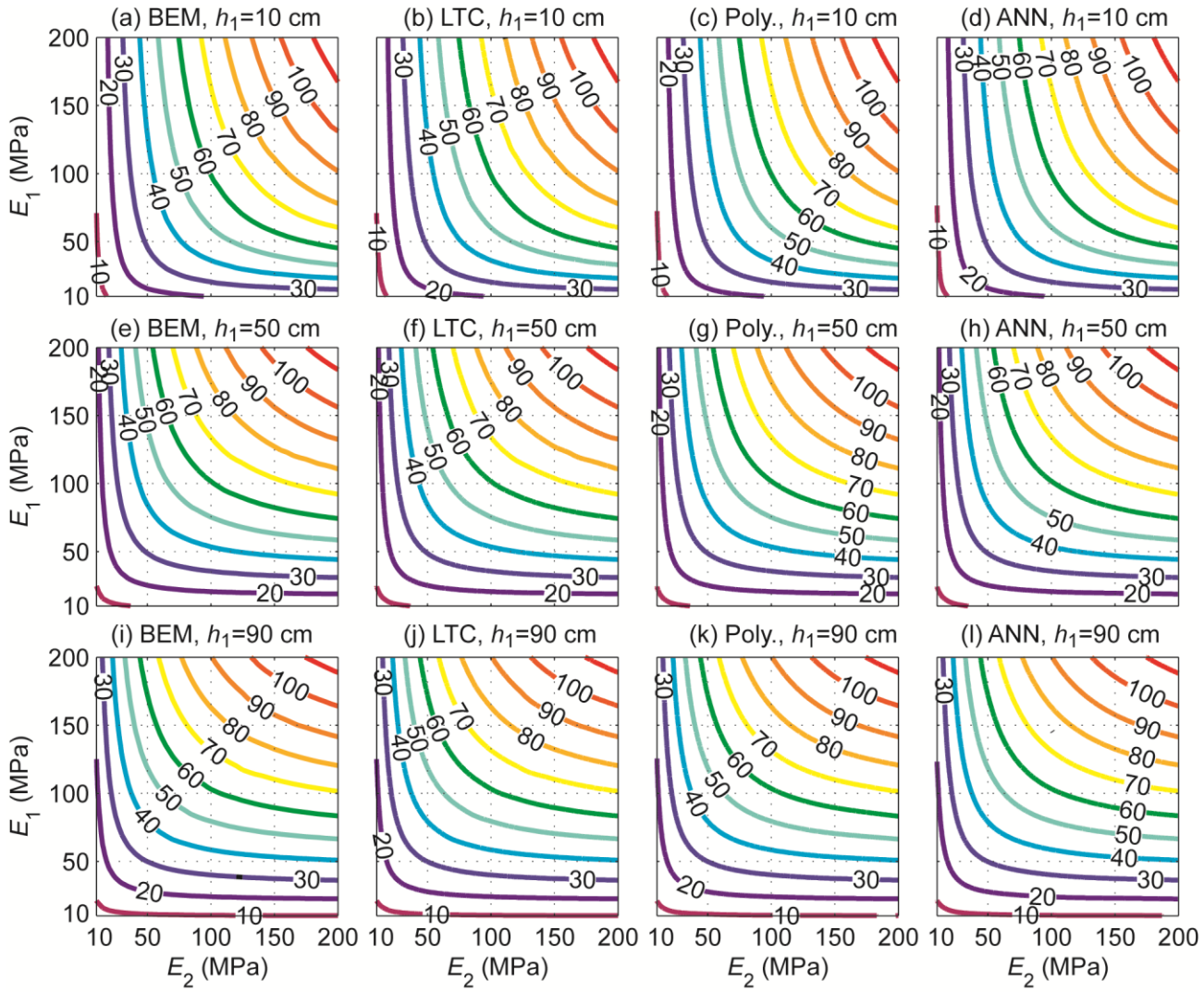

FIGURE 23: Simulated *k* as a function of E_1, E_2 and h_1 from (a) BE analysis and regression models: (b) Database with local interpolation, (c) polynomial fit, and (d) ANN

TABLE 4: Error in *k* (%) between the regression models and BE results

	Percentile				
Model	50	90	95	99	100
LTC	0.02	0.21	0.34	0.77	2.32
Poly	0.09	0.25	0.32	0.57	1.98
ANN	0.12	0.37	0.56	1.10	4.93

The computation time for each model over the entire test set (26,000 simulations) is shown in Table 5. This number of simulation is on the level needed to invert an entire roller data map. The BE model run time of approximately 8 days shows the futility in inverting roller maps using the BE model directly without significantly more computational power. Each of the other models provides a significant decrease in run time, by 6 magnitudes. Thus, these models allow for the possibility of real time inversion.

TABLE 5: Run time over test set (Table 1) which has 26,000 simulations

Model	Total Time	Time Per Simulation
BE	~8 days [1]	~30 sec [2]
Database	0.4 sec	15 μsec [1]
Linear	0.4 sec	15 μsec [1]
ANN	0.4 sec	15 μsec [1]

[1] Computed value based on number of simulations
[2] Time is variable

Back-calculation of top layer modulus E_1 was performed using the three regression-based forward models. For back-calculation with the LTC database and ANN forward models, the secant method with a convergence limit of 0.001 MPa was used, while a Newton-Raphson method with a convergence limit of 0.001 MPa was employed for the 9th order polynomial model. The Newton-Raphson method is similar to the secant method but uses analytical derivatives that can be readily determined for the polynomial model. The error in back-calculated E_1 for various percentiles of the data is summarized in Table 6. The LTC database method yielded the lowest maximum error of 4%, though when considering the 99th percentile, the 9th order polynomial method performs better than the LTC database method. The ANN methods perform well when considering the 95th percentile, with error of 1.5%. However, the ANN method exhibits high maximum errors.

The error in back-calculated E_1 for the regression models shows the influence of the sensitivities in accurately predicting E_1. For the forward models, the LTC and polynomial exhibited the same maximum error (Table 6), but for the back-calculation the polynomial maximum error was three times as large at the LTC. This difference is caused by the change in the sensitivity $\partial E_1/\partial k$ over the space. Thus, the errors in the polynomial model occur where the sensitivity $\partial E_1/\partial k$ is high or conversely the LTC model errors occur where the sensitivity $\partial E_1/\partial k$ is low. When evaluating back-calculation, it is necessary to consider both the errors in the forward model and the sensitivity $\partial E_1/\partial k$.

TABLE 6: Error in back-calculated E_1 (%) using regression models

	Percentile				
Model	50	90	95	99	100
LTC	0.04	0.38	0.68	1.59	4.33
Poly	0.16	0.49	0.65	1.32	11.96
ANN	0.21	0.78	1.30	3.18	21.01

5 PLANS FOR IMPLEMENTATION

The methodology developed through this investigation can in theory be used with all currently-available vibratory IC roller stiffness values. The methodology can be implemented via software algorithms that can be integrated into any commercially available IC software offered by roller manufacturers, consultants and third-party vendors, e.g., navigation system providers. IC software is used on-board the roller and/or on mobile and desktop computers. Therefore, the implementation of the methodology would be performed by the IC software companies. Alternatively, software algorithms could be employed independent of existing IC software. In this approach, the IC data (composite soil stiffness and GPS coordinates) from commercially-available software would be fed into a separate program that would provide layer moduli. The implementation of this approach could be performed by any interested party.

Our efforts to contribute to implementation include distributing this final report and supporting documentation to the various stakeholders who can put this knowledge into practice. These stakeholders include the roller manufacturers, (e.g., Bomag, Ammann, Case, Caterpillar, Dynapac, Hamm, Sakai, Volvo), third party providers of IC equipment (e.g., Trimble), engineering consultants involved in IC, state DOTs and FHWA. Dissemination of the methodology to state DOTs is particularly important because they can drive technology adoption through the implementation of specifications. For example, if specifications require layer or lift based measurement of elastic stiffness or modulus, then there is motivation to implement the methodology developed through this investigation.

6 CONCLUSIONS

In this investigation a methodology was developed to extract layer elastic modulus/stiffness from currently available IC data, i.e., composite soil stiffness and GPS coordinates from vibratory IC rollers. This provides an approach to measure layer based earthwork parameters using IC roller data. The investigation focused on two critical aspects of the methodology, namely, forward modeling and real-time inverse analysis. Forward modeling was pursued via FE and BE based approaches. Both approaches were successful in explaining the relative influence of layer properties (layer modulus and layer thickness) on roller-measured composite soil stiffness. Forward model results matched relatively well with available experimental data. Inverse analysis was pursued with a traditional gradient approach that proved successful but time-intensive when using the FE or BE forward models. As a result, inverse analysis using FE or BE forward models cannot provide real-time back-calculation of layer moduli using current computing power.

The development and use of a statistical regression analysis proved successful in capturing the essence of the FE and BE results and in enabling real-time inverse analysis to estimate layer modulus values. Three different regression models were found to be successful in predicting the FE and BE results (less than 3% error for 99% of the data). Of the three methods, the database with local tri-cubic interpolation provided the lowest overall error.

The ability to back-calculate layer modulus is influenced by measurement error (uncertainty) and parameter sensitivity. The investigation revealed that uncertainty in back-calculated layer modulus increases as the top layer thickness h_1 decreases and/or as the layer modulus ratio E_1/E_2 increases. For commonly-used 15 cm thick lifts of aggregate base course over softer subgrade or subbase soil, the uncertainty in back-calculated base modulus can reach 50% as a direct result of typical IC data measurement error.

The developed methodology can be implemented in practice through software algorithms. These algorithms can be integrated directly into the IC equipment on-board an IC roller, within office software that analyzes IC data, or both. The methodology generated is generic and can be applied to any currently-available proprietary measures of ground stiffness from vibratory rollers. The methodology developed from this investigation will allow all transportation stakeholders (owners, consultants, contractors) to directly evaluate the elastic modulus of individual lifts or layers using vibratory IC roller data.

Further research is required in the area of forward modeling to better match field-observed IC roller response on layered soil. The specific areas that require further development include the drum/soil contact interaction, capturing the stress-dependent elastic modulus of the soil, and capturing the material damping in the soil. Furthermore, advances in IC measurement system accuracy, including GPS-based roller position, are needed to reduce the uncertainty in back-calculated layer modulus. Lastly, the methodology will benefit from implementation and verification on new construction and rehabilitation projects that span a variety of material types and layer thicknesses.

REFERENCES

1. W. Kröber, R. Floss, W. Wallrath. *Dynamic Soil Stiffness as Quality Criterion for Soil Compaction*. Geotechnics for Roads, Rail Tracks and Earth Structures. A.A. Balkema Publishers, Lisse / Abingdon / Exton (Pa) / Tokyo, 2001.
2. R. Anderegg and K. Kaufmann. Intelligent Compaction with Vibratory Rollers: Feedback Control Systems in Automatic Compaction and Compaction Control. Transportation Research Record, Vol. 1868, 2004, pp.124-134.
3. M.A. Mooney and R.V. Rinehart. Field Monitoring of Roller Vibration during Compaction of Subgrade Soil. J. Geotechnical and Geoenvironmental Engineering, Vol. 133, No. 3, 2007, pp. 257-265.
4. M.A. Mooney and R.V. Rinehart. Instrumentation of a Roller Compactor to Monitor Vibration Behavior during Earthwork Compaction. J. Automation in Construction, Vol. 17, No. 2, 2008, pp. 144-150.
5. R.V. Rinehart, J.R. Berger, and M.A. Mooney. Comparison of stress states and paths: vibratory roller-measured soil stiffness and resilient modulus testing. Transportation Research Record, Vol. 2116, 2009, pp. 8-15.
6. G. Chang, Q. Xu, J. Rutledge, R. Horan, L. Michael, D. White, and P. Vennapusa. *Accelerated Implementation of Intelligent Compaction Technology for Embankment Subgrade Soils, Aggregate Base, and Asphalt Pavement Materials*. Report FHWA-IF-12-002. Federal Highway Administration, Washington D.C. 2011.
7. M.A. Mooney, R.V. Rinehart, D.J. White, P. Vennapusa, N. Facas, and O. Musimbi. *Intelligent Soil Compaction Systems*. NCHRP Report 676. Transportation Research Board, Washington, DC, 178 pp., 2011.
8. M.A. Mooney and D. Adam. Vibratory Roller Integrated Measurement of Earthwork Compaction: An Overview. Proc. 7th Intl. Symp. Field Measurements in Geomechanics, ASCE, Boston, MA, Sept. 24-27 2007.
9. T-S. Yoo, and E.T. Selig. Dynamics of Vibratory-Roller Compaction. Journal of the Geotechnical Engineering Division, ASCE, Vol. 105, No. GT10, 1979, pp. 1211-1231.
10. A. Quibel. Le comportement vibratoire: trait d'union entre le choix des parameters et l'efficacite des rouleaux vibrants. Proc., of the Int. Conf. on Compaction, Session VII Compaction Equipment, *ENPC, LCPC*, Paris, France, 1980, pp. 671-676.
11. W. Kröber. *Untersuchung der dynamischen vorgäge bei der vibrationsverdichtung von böden*. Ph.D. Dissertation, Lehrstuhl und Prüfamt fur Grundbau, Bodenmechanik und Felsmechanik der Technischen Universitäte München, schriftenreihe heft 11, München, Deutschland. 1988.
12. D. Adam. *Flächendeckende dynamische Verdichtungskontrolle (FDVK) mit Vibrationswalzen*. Ph.D. Dissertation, Technische Universität Wien, Fakultät für Bauingenieurwesen, Vienna, Austria. 1996.
13. P. van Susante and M.A. Mooney. Capturing Nonlinear Vibratory Roller Compactor Behavior through Lumped Parameter Modeling. Journal of Engineering Mechanics, ASCE, Vol. 134, No. 8, 2008, pp. 684-693.
14. Facas, N.W., van Susante, P.J. and Mooney, M.A. "Influence of Rocking Motion on the Vibratory Roller-Based Measurement of Soil Stiffness," Journal of Engineering Mechanics, ASCE, Vol. 136, No. 7, 2010, pp. 898-905.
15. O.M. Musimbi. *Experimental and Numerical Investigation of Vibratory Drum Interacting with Layered Elastic Media*. PhD Dissertation, Division of Engineering, Colorado School of Mines, 2011.
16. C.A. Brebbia and J. Dominguez. *Boundary Elements: An Introductory Course*. McGraw-Hill, UK, 1992
17. J.R. Berger. Boundary Element Analysis of Anisotropic Bimaterials with Special Green's Functions. Journal of Engineering Analysis with Boundary Elements, Vol. 14, 1995, pp 123-131.
18. R.V. Rinehart, M.A. Mooney, and J.R. Berger. In-Ground Stress-Strain beneath Center and Edge of Vibratory Roller Compactor. Proc. 1st Intl. Conf. Transportation Geotechnics, Nottingham, U.K., Aug. 25-27, 2008.
19. S. Levasseur, Y. Malécot, M. Boulon, and E. Flavigny. Soil Parameter Identification using a Genetic Algorithm. Intl. Journal for Numerical and Analytical Methods in Geomechanics. Vol. 32, No. 2, 2008, pp.189-213.
20. R. Meier and D. Alexander. Using ANN as a Forward Approach to Back-calculation. Transportation Research Record, Vol. 1570, 1997, pp. 126-133.
21. R. Meier and G. Rix. Backcalculation of Flexible Pavements Moduli using ANN. Transportation Research Record, Vol. 1448, 1994, pp. 75-82.
22. B. Goktepe, E. Agar, and H. Lavm. Advances in Back-calculating the Mechanical Properties of Flexible Pavements. Advances in Engineering Software. Vol. 37, 2006, pp. 421-431.
23. E. Alpaydin. *Introduction to Machine Learning*. The MIT Press, Cambridge, Massachusetts, 2004.